



HAL
open science

Oxygen permeation and dimensional stability under pO₂ gradient of (La,Sr)(Fe, Ga)O₃-delta perovskite membranes

Enrique Juste, Aurélie Julian, Thierry Chartier, P. del Gallo, N. Richet

► To cite this version:

Enrique Juste, Aurélie Julian, Thierry Chartier, P. del Gallo, N. Richet. Oxygen permeation and dimensional stability under pO₂ gradient of (La,Sr)(Fe, Ga)O₃-delta perovskite membranes. 10th International Conference of the European Ceramic Society, Jun 2007, Berlin, Germany. pp.738-742. hal-00282691

HAL Id: hal-00282691

<https://hal.science/hal-00282691>

Submitted on 28 May 2008

HAL is a multi-disciplinary open access archive for the deposit and dissemination of scientific research documents, whether they are published or not. The documents may come from teaching and research institutions in France or abroad, or from public or private research centers.

L'archive ouverte pluridisciplinaire **HAL**, est destinée au dépôt et à la diffusion de documents scientifiques de niveau recherche, publiés ou non, émanant des établissements d'enseignement et de recherche français ou étrangers, des laboratoires publics ou privés.

Oxygen permeation and dimensional stability under pO_2 gradient of (La, Sr)(Fe, Ga) $O_{3-\delta}$ perovskite membranes

E. Juste^{1,2*}, A. Julian^{1,2}, T. Chartier¹, P. Del Gallo², N. Richet²

¹SPCTS, CNRS, ENSCI, 47 avenue Albert Thomas, 87065 Limoges, France

²Air Liquide, Centre de Recherche Claude-Delorme, 1 chemin de la porte des Loges, 78354 Jouy-en-Josas Cedex, France

Abstract

Natural gas conversion into syngas, is very attractive for hydrogen or cleanfuel production and provides a new alternative to oil products.

Reactors using mixed ionic-electronic conducting ceramic membranes have received a great interest for their performance and stability. The heart of this reactor is a multilayer membrane composed of a methane reforming catalyst coated up to an active dense membrane, the all supported by a porous layer.

Materials performance is evaluated by measuring the membrane oxygen ionic conductivity in function of temperature, when membranes are exposed to an oxygen partial pressure gradient.

Mechanical stresses are generated through the membrane thickness because of the difference of the dimensional variation of the opposite faces submitted to a high oxygen partial pressure gradient (air/methane) at working temperature near 900°C.

The $La_{0.8}Sr_{0.2}Fe_{0.7}Ga_{0.3}O_{3-\delta}$ perovskite material was retained for the membrane because of long term stability with low dimensional variation under working conditions.

A few enhancement of the oxygen permeating rate across dense membranes elaborated by tape casting was observed as mean grain size is decreasing.

The coating of the surface of the dense $La_{0.8}Sr_{0.2}Fe_{0.7}Ga_{0.3}O_{3-\delta}$ membrane by a porous layer of $La_{0.8}Sr_{0.2}Fe_{0.7}Ni_{0.3}O_{3-\delta}$ improves oxygen permeation flux. Beside, the $La_{0.8}Sr_{0.2}Fe_{0.7}Ni_{0.3}O_{3-\delta}$ layer allows a good capacity to H_2 conversion (87%).

Keywords: Perovskite membrane, Oxygen permeation flux, H_2 conversion

Introduction

Mixed ionic and electronic conductors (MIEC) are of great academic and industrial interests, for more twenty years, for their potential applications, like electrodes of solid oxide fuel cells (SOFCs), membranes for oxygen separation from air and partial oxidation of methane (POM: $CH_4 + \frac{1}{2} O_2 \leftrightarrow CO + H_2$). For the two last applications, the purpose is to obtain synthesis gas

(mixture of CO and H_2 abbreviated "Syngas") via a specific catalysis layer. "Syngas" is an intermediate in the production of more value-added products and a feedstock for the gas-to-liquid conversion from the natural gas to liquid fuels.

In the case of the selective separation of oxygen from air, the temperature must be higher than 700°C to allow transport of oxygen across the dense membrane. The driving force of this transport is the oxygen partial pressure gradient, and no external electrode circuit is needed [1-2]. Ferrocobaltites were the first materials studied by Teraoka for their oxygen transport properties [3]. For an industrial application, the long term chemical and structural stability at high temperature and across an air/natural gas gradient, a mechanical reliability and a high oxygen permeation rate are very important features for the ceramic membrane materials [4].

Potential materials for membrane-reactors application are perovskite like $La_{(1-x)}Sr_xFe_{(1-y)}Ga_yO_{3-\delta}$, due to their dimensional stability in temperature under oxygen chemical potential gradient [5]. Indeed, the lattice volume of these materials is function of both oxygen pressure (pO_2) and temperature. A high dependence of the thermal expansion coefficient (TEC) with oxygen partial pressure, at working temperature, will induce stresses inside material and can lead to ceramic membrane failure, submitted to an oxygen partial pressure gradient.

This work is focused on the oxygen permeating gas performances of $La_{0.8}Sr_{0.2}Fe_{0.7}Ga_{0.3}O_{3-\delta}$ material (LSFG) presenting a sufficient dimensional and chemical stability at high temperature ($T > 750^\circ C$) and under oxygen chemical potential gradient. Secondly, the influence of a $La_{0.8}Sr_{0.2}Fe_{0.7}Ni_{0.3}O_{3-\delta}$ (LSFN) porous coating on the LSFG dense membrane, on the oxygen permeation and on H_2 conversion was evaluated.

Experimental procedure

Powder synthesis

The perovskite $La_{0.8}Sr_{0.2}Fe_{0.7}Ga_{0.3}O_{3-\delta}$ and $La_{0.8}Sr_{0.2}Fe_{0.7}Ni_{0.3}O_{3-\delta}$ powders, synthesized by spray pyrolysis, were supplied by Pharmacie Centrale de France. The powders were attrition-milled using zirconia ball media in ethanol, in order to obtain a monomodal

Corresponding author. Tel.: +33 5 5545 2225; fax: +33 5 5579 0998
e-mail address: t_chartier@ensci.fr (T. Chartier).

distribution with a mean particle size of 0.3 μm and a surface area of 10 m^2/g .

Characterizations

During attrition-milled, grain size distribution was controlled with a laser granulometer (Malvern Instruments Mastersizer 2000). The phase obtained by heat treatment was qualitatively analysed using X-ray diffraction (XRD). Density values of sintered samples were measured by Archimede method. Microstructures were observed by Scanning Electron Microscope (SEM S-2500, Hitachi).

The oxygen permeation was measured, using a specific device presented in Figure 1, in a temperature range from 750°C to 975°C. A dense 1 mm thick membrane was sealed between two alumina tubes with a Pyrex-based glass to obtain a tight system. Upon opposite faces, gas flow (synthetic air to the bottom and argon to the upper surface) were streamed to create an oxygen partial pressure gradient. Oxygen content in argon sweep gas was monitored using a YSZ-oxygen sensor. In the case of using Ar-3% H_2 stream gas, oxygen permeating flux was measured using a TCD gas chromatograph (Varian CP 3380).

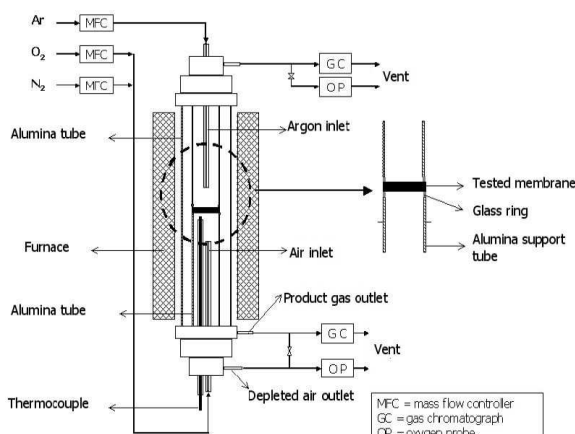


Figure 1: Schematic diagram of oxygen permeation flux measurements system

Membrane: shaping and coating

Dense $\text{La}_{0.8}\text{Sr}_{0.2}\text{Fe}_{0.7}\text{Ga}_{0.3}\text{O}_{3-\delta}$ membranes were shaped by tape casting (Figure 2). A slurry, with an adapted rheological behaviour, was prepared with the addition of a binder and a plasticizer to obtain an acceptable cohesive and flexible green tape.

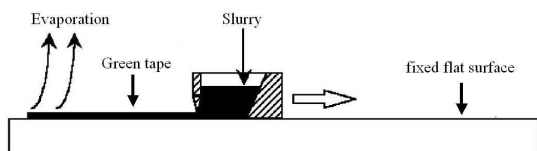


Figure 2: Schematic diagram of tape casting process (Doctor Blade's method)

Disks punched from the green tape were stacked and laminated. Stacks were sintered to obtain 1 mm thick membranes with an apparent density larger than 95%.

A homogeneous $\text{La}_{0.8}\text{Sr}_{0.2}\text{Fe}_{0.7}\text{Ni}_{0.3}\text{O}_{3-\delta}$ paste made from attrition-milled powder mixed with an organic media was coated onto one side surface of $\text{La}_{0.8}\text{Sr}_{0.2}\text{Fe}_{0.7}\text{Ga}_{0.3}\text{O}_{3-\delta}$ sintered dense membranes. The coated membranes were dried at room temperature and heat treatment at 1100°C for 1h, after organic removal. The obtained 90 μm thick layer was porous about with a good adhesion to the dense membrane (Figure 3).

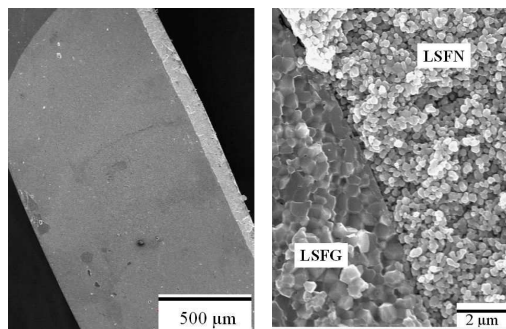
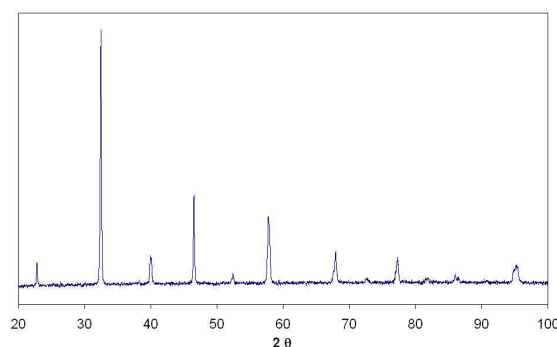


Figure 3: Cross section of $\text{La}_{0.8}\text{Sr}_{0.2}\text{Fe}_{0.7}\text{Ni}_{0.3}\text{O}_{3-\delta}$ (LSFN) coated on $\text{La}_{0.8}\text{Sr}_{0.2}\text{Fe}_{0.7}\text{Ga}_{0.3}\text{O}_{3-\delta}$ (LSFSG) dense membrane.

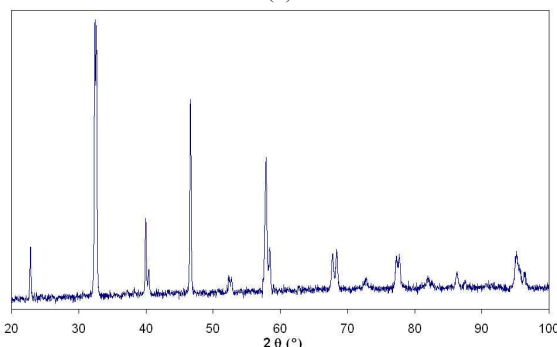
Results and discussions

Structural analysis

Synthesized $\text{La}_{0.8}\text{Sr}_{0.2}\text{Fe}_{0.7}\text{Ga}_{0.3}\text{O}_{3-\delta}$ and $\text{La}_{0.8}\text{Sr}_{0.2}\text{Fe}_{0.7}\text{Ni}_{0.3}\text{O}_{3-\delta}$ powders were controlled by XRD analysis (Figure 4). No impurities are detectable.



(a)



(b)

Figure 4: XRD patterns of $\text{La}_{0.8}\text{Sr}_{0.2}\text{Fe}_{0.7}\text{Ga}_{0.3}\text{O}_{3-\delta}$ (a) and $\text{La}_{0.8}\text{Sr}_{0.2}\text{Fe}_{0.7}\text{Ni}_{0.3}\text{O}_{3-\delta}$ (b) powders.

Oxygen permeation

The permeating oxygen gas flux through the membrane was defined as follows:

$$j_{O_2} = \frac{C \times F}{S} \times \alpha \quad \text{with} \quad \alpha = \frac{P_{\text{measured}} \times T_{\text{(STP)}}}{P_{\text{(STP)}} \times T_{\text{measured}}} \quad (1)$$

where:

j_{O_2} : Oxygen permeation flux through membrane ($\text{Nm}^3/\text{m}^2/\text{h}$)

C : Oxygen amount measured (ppm)

F : Carrier gas output flow (argon) (m^3/h)

S : Membrane effective reacting area (m^2);

$$S = 2,83 \cdot 10^{-4} \text{m}^2$$

α : Normal volume coefficient ;

$$(T_{\text{(STP)}} = 298 \text{ K}; P_{\text{(STP)}} = 10^5 \text{ Pa})$$

Influence of the microstructure

Several studies have demonstrated an influence of membrane microstructure on oxygen permeation flux [6-8]. Two dense membranes were sintered under different conditions (Tab.1) to obtain different grain size distribution (Fig. 5).

Sintering conditions	Relative density	Average grain size (μm)
1250°C / 2h	99 %	0.47
1350°C / 10h	98 %	0.95

Table 1: Sintering conditions and associated mean grain size of $\text{La}_{0.8}\text{Sr}_{0.2}\text{Fe}_{0.7}\text{Ga}_{0.3}\text{O}_{3-\delta}$ membrane.

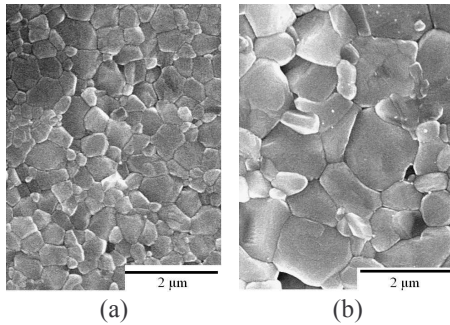


Figure 5: SEM micrographs of $\text{La}_{0.8}\text{Sr}_{0.2}\text{Fe}_{0.7}\text{Ga}_{0.3}\text{O}_{3-\delta}$ sintered, (a) 1250°C for 2h and (b) 1350°C for 10h.

The membrane with the finest microstructure, then with the highest grain boundary density, presents the largest oxygen permeation flux (Fig.6) with a factor 1.7 for a factor 2 of mean grain size. Oxygen permeation flux increase with temperature. That can be explained by an enhancement of oxygen vacancies concentration and their mobility with temperature [9].

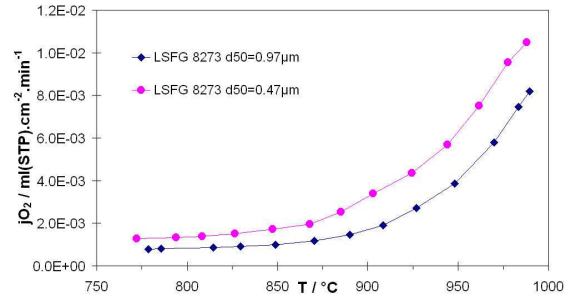


Figure 6: Evolution of oxygen permeation flux of $\text{La}_{0.8}\text{Sr}_{0.2}\text{Fe}_{0.7}\text{Ga}_{0.3}\text{O}_{3-\delta}$ with temperature for 2 grain size distributions (air/Ar gradient).

Influence of the surface coating with LSFN on oxygen permeation

The permeating oxygen gas through LSFSG dense membrane coated with a porous LSFN layer was measured in a air/Ar gradient (Fig. 7 and 8), then in a air/(Ar-3% H_2) gradient. The LSFN layer was placed in the low oxygen partial pressure side.

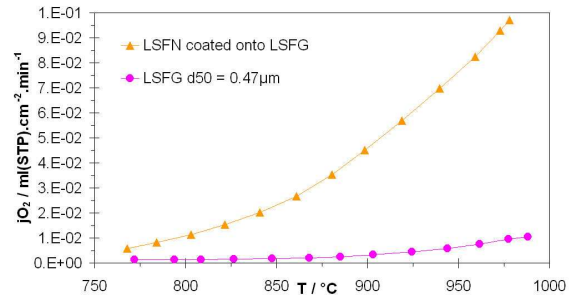


Figure 7: Evolution of oxygen permeation flux through $\text{La}_{0.8}\text{Sr}_{0.2}\text{Fe}_{0.7}\text{Ga}_{0.3}\text{O}_{3-\delta}$ dense membrane coated with a porous $\text{La}_{0.8}\text{Sr}_{0.2}\text{Fe}_{0.7}\text{Ni}_{0.3}\text{O}_{3-\delta}$ layer in air/Ar gradient.

In the temperature measurement range, oxygen permeation flux for LSFN coated-dense membrane is significantly higher than LSFSG dense membrane. At 775°C, oxygen permeation through coated membrane is 4 times larger than uncoated one. The oxygen permeating gas was 0.0056 and 0.0013 $\text{ml}/\text{cm}^2/\text{min}$ for LSFN/LSFSG and LSFSG membranes, respectively at 775°C. At 980°C, this difference is multiplied by a factor nearly 10, j_{O_2} was 0.097 and 0.010 $\text{ml}/\text{cm}^2/\text{min}$ for LSFN/LSFSG and LSFSG membranes, respectively. This significant enhancement of the oxygen flux can be explained both by an extension of the effective surface area and by the catalyst effect of $\text{La}_{0.8}\text{Sr}_{0.2}\text{Fe}_{0.7}\text{Ni}_{0.3}\text{O}_{3-\delta}$ coating to the oxygen desorption [10]. These results show that a significant change occurred at the membrane / Ar interface with the $\text{La}_{0.8}\text{Sr}_{0.2}\text{Fe}_{0.7}\text{Ni}_{0.3}\text{O}_{3-\delta}$ coating.

Oxygen transport through dense membrane is function of thermally activated mechanisms, so it is useful to represent flux data, from the point of view of activation energy. Arrhenius plots of oxygen permeation fluxes, as a function of the inverse temperature, is presented in Figure 8. For the two membranes type, in the temperature range studied, the slopes, then the apparent activation energy, change. This variation of slope was reproducible with thermally cycles. This can be explained by an evolution of the limiting step in oxygen

transport through the membrane [7-10]. The same activation energy was calculated for the LSFN membranes with the two different microstructures. At low temperature ($T < 870^\circ\text{C}$), the apparent activation energy (E_a) is equal to 45 kJ/mol and at high temperature ($T > 870^\circ\text{C}$), $E_a = 169$ kJ/mol. In the case of LSFN/LSFG, apparent activation energy is equal to 156 kJ/mol at low temperature and to 116 kJ/mol at high temperature. For temperatures above 870°C , the presence of the LSFN layer allows to decrease the activation energy of about 50 kJ/mol. A similar behaviour of activation energy for LSFN/LSFG between low and high temperature was observed by Lee et al. for LaSrGaFeO_3 membranes surface modified by LaSrCoO_3 [10]. These results suggest that, for temperatures above 870°C , oxygen permeation flux was mainly governed by surface limitation exchanges. Below 870°C , bulk oxygen transport was dominant.

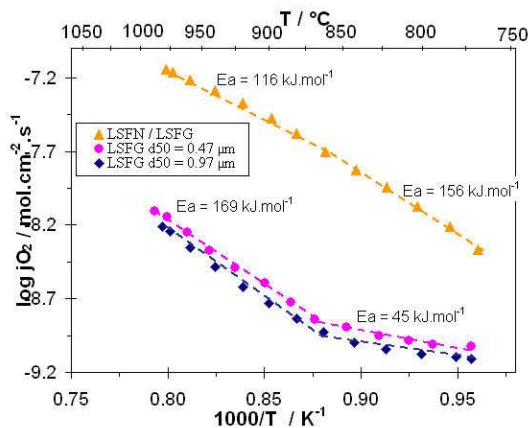


Figure 8: Arrhenius plots of oxygen permeation of $\text{La}_{0.8}\text{Sr}_{0.2}\text{Fe}_{0.7}\text{Ga}_{0.3}\text{O}_{3-\delta}$ dense membrane coated with $\text{La}_{0.8}\text{Sr}_{0.2}\text{Fe}_{0.7}\text{Ni}_{0.3}\text{O}_{3-\delta}$ and $\text{La}_{0.8}\text{Sr}_{0.2}\text{Fe}_{0.7}\text{Ga}_{0.3}\text{O}_{3-\delta}$ dense membranes in air/Ar gradient.

Influence of the LSFN coating on H_2 conversion

To assess H_2 conversion capacity of $\text{La}_{0.8}\text{Sr}_{0.2}\text{Fe}_{0.7}\text{Ni}_{0.3}\text{O}_{3-\delta}$ coating, a conversion test was performed with an air/(Ar-3% H_2) gradient. Synthetic air was feed onto the dense LSFN uncoated surface, and input flow of (Ar-3% H_2) was swept the LSFN coating. Reaction 2 takes place on the LSFN surface and H_2 content in the output flow was measured (Fig.9).



The conversion of H_2 was defined as follow:

$$\text{H}_2\text{conversion}(\%) = \frac{H_2(\text{in}) - H_2(\text{out})}{H_2(\text{in})} \times 100 \quad (3)$$

No significant conversion was observed for LSFN dense membrane.

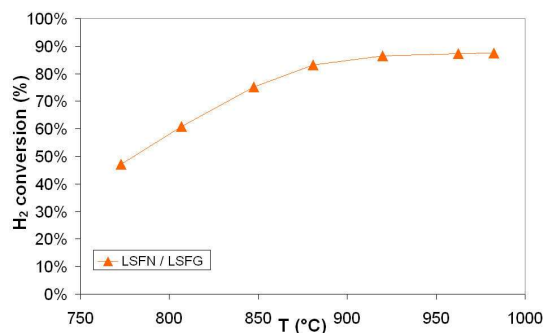


Figure 9: H_2 conversion of $\text{La}_{0.8}\text{Sr}_{0.2}\text{Fe}_{0.7}\text{Ga}_{0.3}\text{O}_{3-\delta}$ dense membrane coated with porous $\text{La}_{0.8}\text{Sr}_{0.2}\text{Fe}_{0.7}\text{Ni}_{0.3}\text{O}_{3-\delta}$ layer in air/(Ar-3% H_2) gradient.

H_2 conversion increases with temperature up to 87.5% . A steady state seems reached near 900°C .

In order to improve LSFN coating, it would be interesting to study dependence of coating surface area with performance under air/(Ar-3% H_2) and air/methane gradient.

Conclusion

A decrease of oxygen permeation flux performances was observed as the mean grain size of $\text{La}_{0.8}\text{Sr}_{0.2}\text{Fe}_{0.7}\text{Ga}_{0.3}\text{O}_{3-\delta}$ dense-membrane is increasing.

The coating of $\text{La}_{0.8}\text{Sr}_{0.2}\text{Fe}_{0.7}\text{Ga}_{0.3}\text{O}_{3-\delta}$ dense-membrane by a porous $\text{La}_{0.8}\text{Sr}_{0.2}\text{Fe}_{0.7}\text{Ni}_{0.3}\text{O}_{3-\delta}$ layer allows to improve the oxygen permeation and modifies the limiting step of oxygen transport with the reduction of the activation energy at temperature above 870°C .

The H_2 conversion capacity of the LSFN coated LSFN membrane reaches 87% in air/(Ar-3% H_2) gradient.

References

1. A. Sammells, F. Anthony, M. Schwartz et al: Catalytic membrane reactors for spontaneous synthesis gas production. *Catalysis Today* **56** (2000), 325–328.
2. U. Balachandran, J. T. Dusek, R. L. Mieville et al: Dense ceramic membranes for partial oxidation of methane to syngas. *Applied Catalysis A: General* **133**, **1** (1995) 19-29.
3. Y. Teraoka, H.M. Zhang, S. Furukawa, N. Yamazoe: Oxygen permeation through perovskite-type oxides. *Chemistry Letters* (1985) 1743–1746.
4. V.V. Kharton, A. A. Yaremchenko, M. V. Patrakeev et al: Thermal and chemical induced expansion of $\text{La}_{0.3}\text{Sr}_{0.7}(\text{Fe,Ga})\text{O}_{3-\delta}$ ceramics. *Journal of the European Ceramic Society* **23** (2003). 1417–1426.

5. V.V. Kharton, A.L. Shaulo, A. P. Viskup, M. Avdeev et al: Perovskite-like system (Sr,La)(Fe,Ga)O_{3-δ}: structure and ionic transport under oxidizing conditions. *Solid State Ionics*. **150** (2002), 229–243.
6. V. V. Kharton, E. N. Naumovich, A. V. Kovalevsky et al: Mixed electronic and ionic conductivity of LaCo(M)O₃ (M=Ga, Cr, Fe or Ni): IV. Effect of preparation method on oxygen transport in LaCoO_{3-δ}. *Solid State Ionics*. **138** (2000) 135-148
7. Diethelm, J. Van herle, J. Sfeir et al: Correlation between oxygen transport properties and microstructure in La_{0.5}Sr_{0.5}FeO_{3-δ}. *Journal of the European Ceramic Society* **25** (2005) 2191-2196.
8. G. Etchegoyen, T. Chartier, A. Julian et al : Microstructure and oxygen permeability of a La_{0.6}Sr_{0.4}Fe_{0.9}Ga_{0.1}O_{3-δ}] membrane containing magnesia as dispersed second phase particles. *Journal of Membrane Science* **268** (2006) 86-95.
9. G. Etchegoyen: Développement d'une membrane céramique conductrice mixte pour la production de gaz de synthèse. Phd thesis, Limoges University, France (2005).
10. S. Lee, K. S. Lee, S. K. Woo et al: Oxygen-permeating property of LaSrBFeO₃ (B=Co, Ga) perovskite membrane surface-modified by LaSrCoO₃. *Solid State Ionics* **158** (2003), 287-296.